

7. Penn, A. A., Riquelme, P. A., Feller, M. B. & Shatz, C. J. Competition in retinogeniculate patterning driven by spontaneous activity. *Science* **279**, 2108–2112 (1998).
8. Cynader, M., Berman, N. & Hein, A. Cats reared in stroboscopic illumination: effects on receptive fields in visual cortex. *Proc. Natl Acad. Sci. USA* **70**, 1353–1354 (1973).
9. Schmidt, J. T. & Eisele, L. E. Stroboscopic illumination and dark rearing block the sharpening of the regenerated retinotectal map in goldfish. *Neuroscience* **14**, 535–546 (1985).
10. Weliky, M. & Katz, L. C. Disruption of orientation tuning in visual cortex by artificially correlated neuronal activity. *Nature* **386**, 680–685 (1997).
11. Sharma, J., Angelucci, A. & Sur, M. Induction of visual orientation modules in auditory cortex. *Nature* **404**, 841–847 (2000).
12. von Melchner, L., Pallas, S. L. & Sur, M. Visual behaviour mediated by retinal projections directed to the auditory pathway. *Nature* **404**, 871–876 (2000).
13. Fregnac, Y., Shulz, D., Thorpe, S. & Bienenstock, E. A cellular analogue of visual cortical plasticity. *Nature* **333**, 367–370 (1988).
14. Schuett, S., Bonhoeffer, T. & Hubener, M. Pairing-induced changes of orientation maps in cat visual cortex. *Neuron* **32**, 325–337 (2001).
15. Gaze, R. M., Keating, M. J. & Chung, S. H. The evolution of the retinotectal map during development in *Xenopus*. *Proc. R. Soc. London B* **185**, 301–330 (1974).
16. Holt, C. E. & Harris, W. A. Order in the initial retinotectal map in *Xenopus*: a new technique for labelling growing nerve fibres. *Nature* **301**, 150–152 (1983).
17. Markram, H., Lübke, J., Frotscher, M. & Sakmann, B. Regulation of synaptic efficacy by coincidence of postsynaptic APs and EPSPs. *Science* **275**, 213–215 (1997).
18. Zhang, L., Tao, H. W., Holt, C. E., Harris, W. A. & Poo, M. M. A critical window for cooperation and competition among developing retinotectal synapses. *Nature* **395**, 37–44 (1998).
19. Feldman, D. E. Timing-based LTP and LTD at vertical inputs to layer II/III pyramidal cells in rat barrel cortex. *Neuron* **27**, 45–56 (2000).
20. Boettiger, C. A. & Doupe, A. J. Developmentally restricted synaptic plasticity in a songbird nucleus required for song learning. *Neuron* **31**, 809–818 (2001).
21. Abbott, L. F. & Blum, K. I. Functional significance of long-term potentiation for sequence learning and prediction. *Cereb. Cortex* **6**, 406–416 (1996).
22. Zanker, J. M. & Zeil, J. *Motion Vision—Computational, Neural, and Ecological Constraints* (Springer, New York, 2000).
23. Rao, R. P. & Sejnowski, T. J. Predictive learning of temporal sequences in recurrent neocortical circuits. *Novartis Found. Symp.* **239**, 208–229 (2001).
24. Roberts, P. D. Computational consequences of temporally asymmetric learning rules. I. Differential hebbian learning. *J. Comput. Neurosci.* **7**, 235–246 (1999).
25. Mehta, M. R., Barnes, C. A. & McNaughton, B. L. Experience-dependent, asymmetric expansion of hippocampal place fields. *Proc. Natl Acad. Sci. USA* **94**, 8918–8921 (1997).
26. Mehta, M. R., Quirk, M. C. & Wilson, M. A. Experience-dependent asymmetric shape of hippocampal receptive fields. *Neuron* **25**, 707–715 (2000).
27. Bliss, T. V. P. & Collingridge, G. L. A synaptic model of memory: long-term potentiation in the hippocampus. *Nature* **361**, 31–39 (1993).
28. Malenka, R. C. & Nicoll, R. A. Long-term potentiation—a decade of progress? *Science* **285**, 1870–1874 (1999).
29. Zhang, L., Tao, H. & Poo, M. Visual input induces long-term potentiation of developing retinotectal synapses. *Nature Neurosci.* **3**, 708–715 (2000).
30. Rae, J., Cooper, K., Gates, P. & Watsky, M. Low access resistance perforated patch recordings using amphotericin B. *J. Neurosci. Methods* **37**, 15–26 (1991).

Acknowledgements

This work was supported by grants from NSF and NIH. F.E. was supported in part by a long-term fellowship from the Human Frontier Science Program.

Competing interests statement

The authors declare that they have no competing financial interests.

Correspondence and requests for materials should be addressed to M.-m.P. (e-mail: mpoo@uclink.berkeley.edu).

Dendrite growth increased by visual activity requires NMDA receptor and Rho GTPases

Wun Chey Sin, Kurt Haas, Edward S. Ruthazer & Hollis T. Cline

Cold Spring Harbor Laboratory, Cold Spring Harbor, New York 11724, USA

Previous studies suggest that neuronal activity may guide the development of synaptic connections in the central nervous system through mechanisms involving glutamate receptors and GTPase-dependent modulation of the actin cytoskeleton^{1–7}. Here we demonstrate by *in vivo* time-lapse imaging of optic tectal cells

in *Xenopus laevis* tadpoles that enhanced visual activity driven by a light stimulus promotes dendritic arbor growth. The stimulus-induced dendritic arbor growth requires glutamate-receptor-mediated synaptic transmission, decreased RhoA activity and increased Rac and Cdc42 activity. The results delineate a role for Rho GTPases in the structural plasticity driven by visual stimulation *in vivo*.

We used *in vivo* time-lapse imaging of single optic tectal neurons in *Xenopus* tadpoles to test the function of visual activity in neuronal development. We compared the dendritic arbor growth rates of individual tectal neurons during a 4-h period with a visual stimulus to a preceding 4-h period in the absence of light. This imaging protocol allows the comparison of dendritic arbor structures of the same neurons over time and therefore provides a sensitive measure of structural plasticity. Visual stimulation significantly enhanced dendritic arbor elaboration compared with growth rates in the preceding 4-h period in the dark (Fig. 1a, b; see also Supplementary Table 1). Neurons from animals exposed to visual stimulus throughout the 8-h protocol maintained a constant rate of dendritic arbor elaboration (Fig. 1b; see also Supplementary Fig. 1 and Table 1). This indicates that growth rates do not change with longer periods of stimulation. Another set of animals was exposed to visual stimulus within the first 4-h period and then returned to the dark

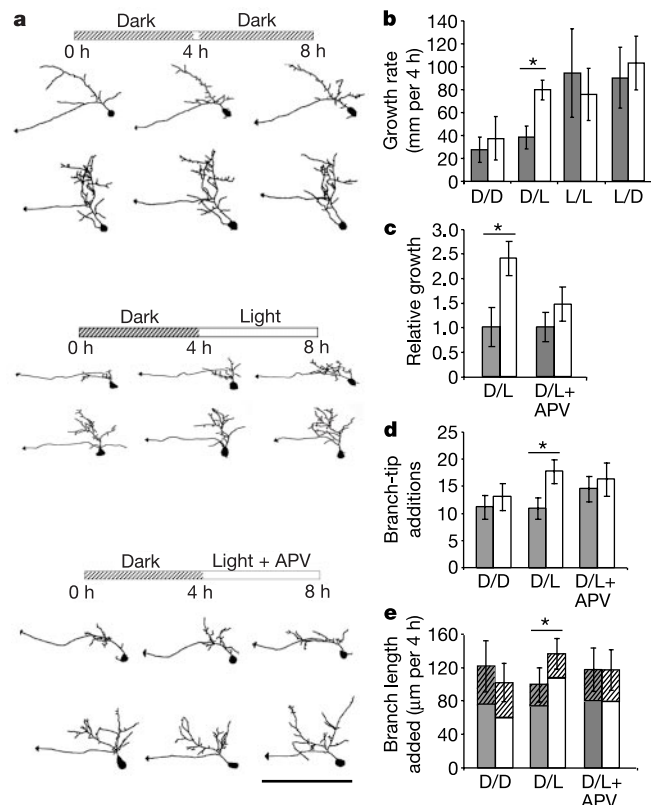


Figure 1 Visual stimulation *in vivo* promotes dendritic arbor growth by a glutamate-receptor-dependent mechanism. **a**, Drawings of neurons imaged three times at 4-h intervals. Two examples are shown for each treatment. Animals were placed in a dark chamber for 4 h (dark) or a chamber with a light stimulus for 4 h (light) in the presence or absence of APV as depicted by the bar over the neurons. Arrowheads identify efferent axons in this and subsequent figures. Scale bar, 100 μm. **b**, Quantification of dendritic arbor growth rates during 4 h in the dark (D) or with visual stimulation (L). **c**, Dendritic arbor growth rates normalized to the growth rate in the 0–4 h period in the dark (D). **d**, Quantification of branch-tip additions. **e**, Contribution of new branches or branch extension (hatched, top region) to increased branch length. Asterisk, $P < 0.05$.

for the second 4-h period. Notably, the enhanced growth rates of these neurons in response to light stimulation were maintained during the 4-h dark period (Fig. 1b; see also Supplementary Fig. 1). This suggests that exposure to visual stimulation triggers mechanisms that enhance dendritic arbor growth over a period following termination of the stimulus.

Although the experimental protocol was designed to detect

structural changes within individual neurons, we also detect a significant increase in the growth rate of neurons from animals exposed to visual stimulation during the first 4 h of the experiment ($68.3 \pm 12.1 \mu\text{m}$, $n = 16$) compared with the growth rate of neurons from animals placed in the dark for the initial 4 h ($35.4 \pm 6.0 \mu\text{m}$, $n = 84$, $P < 0.002$). This indicates that the increased growth rate is due to the visual stimulus rather than

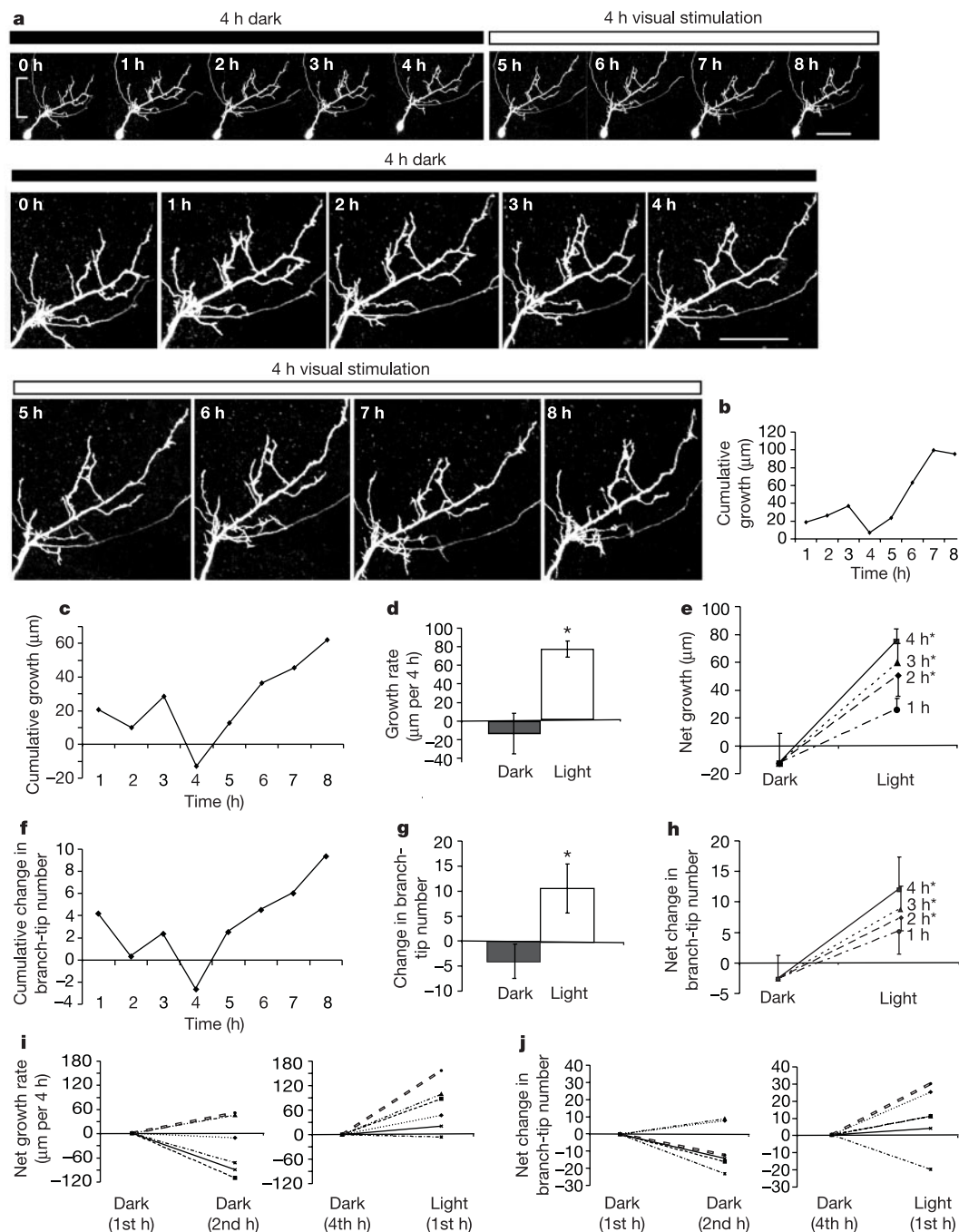


Figure 2 Visual system activity regulates branch dynamics *in vivo*. **a**, Two-photon images of a neuron collected once an hour over 8 h, during a visual stimulus regime depicted by the bars over the images. The bottom two panels show greater magnification of the bracketed region in the top panel. Scale bars, $50 \mu\text{m}$. **b**, Cumulative change in branch length for the neuron in **a**. **c**, **f**, Average cumulative change in branch length (**c**) and branch-tip number (**f**) ($n = 6$); **d**, **g**, Average change in branch length (**d**) and branch-tip number (**g**) over the 4-h period in the dark (dark) or with visual stimulus (light).

e, **h**, Cumulative change in branch length (**e**) and branch-tip number (**h**) with each hour of visual stimulus (light) compared with 4 h without visual stimulus (dark). **i**, **j**, Changes in branch length (**i**) and branch-tip number (**j**) for individual neurons from the first to second hours in the dark (left graphs) compared with changes during the last hour in the dark and first hour with visual stimulation (right graphs). Asterisk, $P < 0.05$.

a reaction to the 4 h in the dark.

The light-induced increase in dendritic arbor growth rate was blocked by exposure to APV (3-amino-phosphonovaleric acid; Fig. 1a, c) and CNQX (6-cyano-nitroquinoxaline-2,3-dione; Supplementary Fig. 1) during visual stimulation. These antagonists block NMDAR (*N*-methyl-D-aspartate receptors) and AMPAR (α -amino-3-hydroxy-5-methyl-4-isoxazolepropionate receptors), respectively. Therefore glutamate-receptor-dependent signalling is necessary for light-induced arbor elaboration.

Dendritic arbors grow through the selective stabilization of a fraction of newly added branches and the extension of those branches^{7–9}. Visual stimulation significantly increased the number of new branches detected after 4 h (Fig. 1d, e; see also Supplementary Table 2). APV blocked the light-induced increase in branch additions and increased the rate of branch retractions (Fig. 1d; see also Supplementary Table 2). Newly added branches account for the increased branch length seen with light stimulation (Fig. 1e). Total branch length from branch additions and extensions is significantly greater when animals are exposed to light, compared with dark or compared with animals exposed to light in the presence of APV. The data indicate that visual stimulation enhances arbor growth by stabilizing newly added branches and suggest a role of NMDA receptors in activity-induced branch initiation and stabilization.

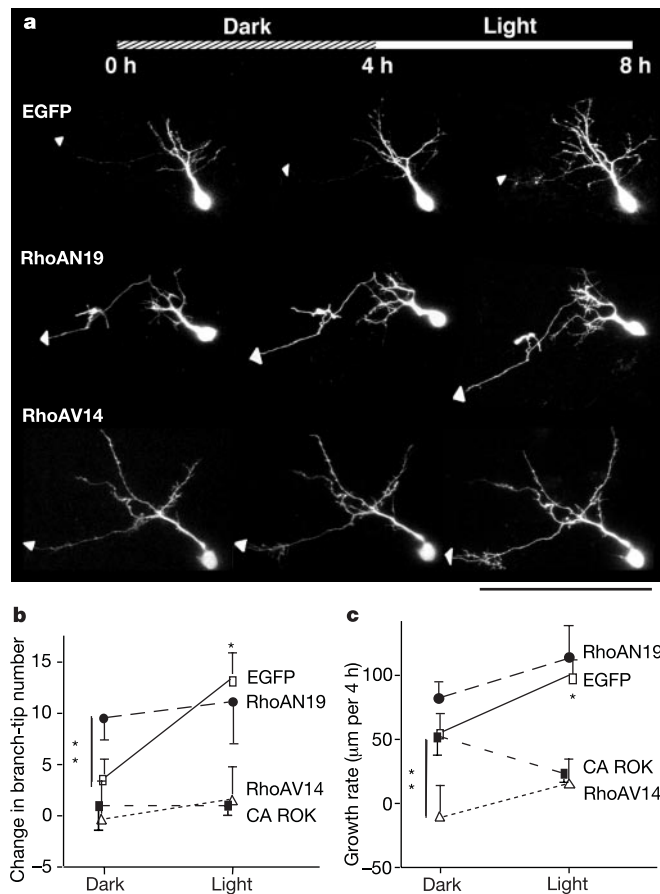


Figure 3 Decreased RhoA activity mediates light-induced dendritic arbor growth. **a**, Time-lapse *in vivo* confocal images collected at 4-h intervals over 8 h of tectal neurons expressing EGFP, dominant-negative RhoA (RhoAN19) or constitutively active (CA) RhoA (RhoAV14). Scale bar, 100 μm. **b**, **c**, Change in branch-tip number (**b**) and branch length (**c**) over 4 h in the dark (dark) or with visual stimulation (light). Asterisk, $P < 0.05$, Wilcoxon signed-rank test; double asterisk, $P < 0.05$, Mann–Whitney *U*-test.

The time course of the effect of visual stimulation on dendritic arbor dynamics was analysed by collecting two-photon microscope images of individual green fluorescent protein (GFP)-expressing tectal neurons at 1-h intervals over a period of 8 h (Fig. 2a). This stimulation and imaging protocol led to a significant light-induced increase in dendritic arbor growth rate and branch-tip number (Fig. 2d, g), as seen when animals were imaged three times over 8 h (Fig. 1). Despite the continuous addition and retraction of branches throughout 8 h (Fig. 2c, f), arbors showed a net increase in growth rate and branch-tip number during light stimulation, but not over

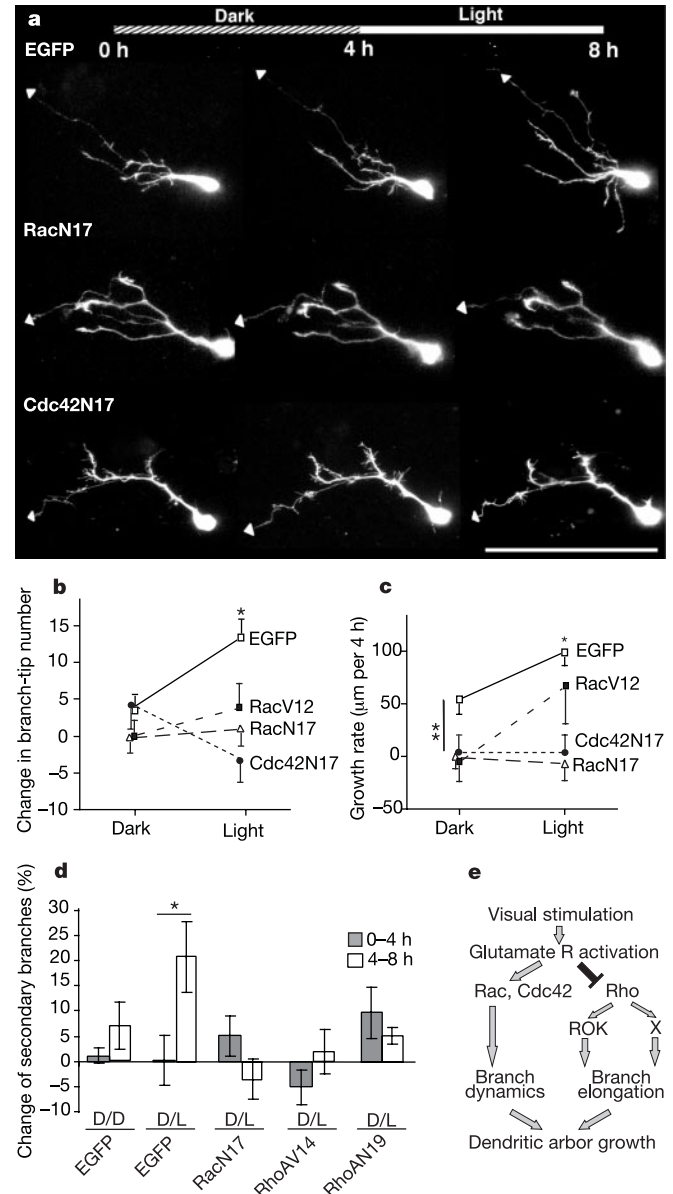


Figure 4 Rac and Cdc42 mediate the light-induced increase in dendrite branch number. **a**, Time-lapse *in vivo* confocal images of tectal neurons expressing EGFP, dominant-negative Rac (RacN17) or dominant-negative Cdc42 (Cdc42N17) over 8 h. Scale bar, 100 μm. **b**, **c**, Change in branch-tip number (**b**) and dendritic branch length (**c**) over 4 h in the dark (dark) or with visual stimulation (light). **d**, Change in secondary dendritic branches (expressed as per cent of initial total branch number) added to the primary dendrite during 4 h in the dark (D) or with visual stimulation (L) in neurons expressing the designated constructs. **e**, Summary of the role of visual stimulation and the Rho GTPases in dendritic arbor development (see text for details). Asterisk, $P < 0.05$, Wilcoxon signed-rank test; double asterisk, $P < 0.05$, Mann–Whitney *U*-test.

4 h in the dark (Fig. 2e, h). The change in branch length and branch-tip number is significantly greater by the second hour of visual stimulation than the change seen over 4 h in the dark. Five out of six neurons increased branch-length growth rates and branch-tip number in the first hour of visual stimulation compared with the previous hour in the dark (Fig. 2i, j). By contrast, most of the neurons decreased growth rates and branch dynamics during the first and second time windows in the dark (Fig. 2i, j). These data indicate that dendritic arbors respond within the first hour to visual stimulation with an increase in branch length and branch-tip number. The continued increase in branch-tip number and branch length with each hour of visual stimulation indicates that the system does not adapt to the visual stimulus over 4 h of visual stimulation.

Neuronal arbor elaboration requires the reorganization of the cytoskeleton. The Rho family of small GTPases regulates actin dynamics¹⁰ and has been implicated in the control of neuronal morphogenesis¹¹. Regulators and effectors of small GTPases such as kalirin-7, SynGAP and citron associate with NMDA receptors, providing potential biochemical links between NMDAR activity and GTPase-mediated regulation of cytoskeletal dynamics^{12–16}. However, no study has yet demonstrated a role for Rho GTPases under physiological conditions that control dendritic arbor development. Therefore we investigated the contribution of the Rho family of GTPases to the signalling mechanisms underlying activity-induced dendritic growth.

We have used recently an *in situ* binding assay to demonstrate that stimulation of the optic nerve significantly decreases endogenous RhoA activity and increases endogenous Rac activity in the optic tectum³. These changes require glutamate receptor activity. Here, we tested whether increased Rac and Cdc42 and decreased RhoA activity are required for light-induced dendritic arbor elaboration by collecting time-lapse images *in vivo* of optic tectal neurons co-expressing GFP and either constitutively active or dominant-negative forms of Rho GTPases. Constitutively active RhoAV14 blocked the light-induced dendritic arbor development that is seen in GFP-expressing neurons (Fig. 3a–c). These data indicate that RhoA activity inhibits activity-dependent dendritic arbor growth. They also suggest that visual stimulation promotes arbor growth by inhibiting RhoA, consistent with previous studies showing that decreased RhoA activity increases dendritic arbor elaboration⁴. If light stimulation activated a parallel pathway promoting dendritic arbor elaboration that is independent of RhoA activity, one would predict a synergistic effect of visual stimulation and expression of dominant-negative RhoAN19; however, light stimulation did not increase further dendritic arbor elaboration induced by dominant-negative RhoAN19 (Fig. 3a–c). This occlusion of light-induced dendritic arbor growth by dominant-negative RhoAN19 suggests that endogenous RhoA activity is relatively high in dendrites with slow growth rates and that decreasing RhoA activity increases dendritic arbor development. Therefore, in combination with our findings that optic nerve stimulation decreases endogenous RhoA activity³, these data suggest that RhoA is a downstream component of the light-induced pathway controlling dendritic arbor elaboration.

RhoA has been reported to negatively regulate dendrite outgrowth through ROK (also known as ROCK), a RhoA-binding kinase¹¹. Other potential RhoA effectors are mDia, protein kinase N, citron kinase, Lim kinase-1 and PRK2 (refs 17, 18). Expression of constitutively active ROK inhibited light-induced dendritic arbor growth (Fig. 3b, c). This suggests that the inhibition of activity-dependent dendritic arbor growth by RhoAV14 is at least partially mediated by enhanced ROK activity, consistent with the idea that light-induced arbor elaboration occurs when both RhoA and ROK activities are low.

Previous experiments⁴ and experiments included here indicate that Rac activity controls rates of branch additions and retractions.

Our *in situ* GTPase assays³ indicate that decreasing Rho activity increases Rac activity. This suggests that the increase in branch-tip number seen with inhibition of RhoA activity is probably due to activation of Rac. These data also suggest that regulation of branch dynamics is affected primarily by Rac activity, and that RhoA can alter Rac-mediated branch dynamics *in vivo*.

Tectal neurons expressing dominant-negative RacN17 and Cdc42N17 failed to respond to light stimulus with the increase in branch-tip number and branch length seen in GFP-expressing (EGFP) neurons (Fig. 4a–c; see also Supplementary Table 3). These data indicate that activation of Rac and Cdc42 is required for increased arbor elaboration in response to visual stimulation. Neurons expressing constitutively active RacV12 failed to show the significant light-induced increase in branch-tip number seen with EGFP controls (Fig. 4b, c). Although this is consistent with our observations that expression of constitutively active RacV12 increases RhoA activity³, which inhibits dendritic arbor growth, we cannot exclude the possibility that cycling of Rac from the GTP-bound to GDP-bound form may be required for its optimum activity¹⁹.

GTPase expression also affects arbor development in the absence of visual stimulation. Constitutively active RhoAV14 inhibited rates of branch additions and dendritic arbor growth in the dark compared with GFP-expressing control neurons ($P < 0.05$, Mann–Whitney *U*-test), whereas constitutively active ROK did not (Fig. 3b, c). Neurons expressing dominant-negative Cdc42N17 or dominant-negative RacN17 had significantly decreased rates of arbor growth and changes in branch-tip number compared with GFP-expressing control neurons ($P < 0.05$; Fig. 4a–c). These neurons could be imaged and appeared healthy for up to 10 days, indicating that expression of these mutants was not toxic. These observations are consistent with previous results^{4,11} and support the idea that the Rho GTPases are positioned at a bottleneck of multiple signal transduction pathways affecting neuronal structure¹¹.

Dendritic arbor development may proceed through repeated branching of dendritic growth cones or through a mechanism called ‘interstitial/back branching’ in which new branches emerge from more stable branches within the arbor²⁰. Tectal projection neurons imaged in this study have a single stable primary dendrite, an average of 12 secondary branches originating from the primary dendrite, and complex arborizations with up to fifth-order branches. Light stimulus significantly increased the number of secondary branches (Fig. 4d), indicating that interstitial branching is a prominent mechanism controlling dendritic arbor elaboration in response to visual stimulation *in vivo*. Expression of dominant-negative RacN17, Cdc42N17, RhoAN19 or constitutively active RhoAV14 prevented the light-induced increase in secondary branches. This indicates that the GTPases regulate the formation of interstitial branches in response to visual stimulation.

Our data indicate that visual system activity affects dendritic arbor elaboration through a mechanism involving Rho GTPases (Fig. 4e). Expression of mutant GTPases that interfere with endogenous GTPases blocks light-induced dendritic arbor development. We suggest that enhanced Rac and Cdc42 activity promotes branch dynamics. Decreased Rho activity promotes branch elongation mediated by several downstream effectors, including ROK. Rac- and Cdc42-mediated branch addition and stabilization and RhoA-mediated branch elongation⁴ cooperate to result in dendritic arbor growth.

Our data demonstrating that NMDAR activity and GTPases are both required for dendritic arbor development suggest that calcium influx through NMDAR affects regulators of Rho GTPase activity. Such regulation may occur through GTPase regulators or effectors such as SynGAP, kalarin or trio^{12,13,16,21}. The Rho GTPases may also affect intracellular calcium levels by regulating calcium influx into cells²² or calcium-induced calcium release from intracellular stores²³. Calcium-dependent events, including calcium- and calmo-

dulin-dependent kinase type II (CaMKII)-mediated branch stabilization²⁴, may cooperate with GTPase-mediated branch initiation and extension to control dendritic arbor development.

Glutamate-mediated synaptic activity is probably one of several regulators that affect dendritic arbor elaboration of tectal cells by activating the Rho GTPases. Several other extracellular signalling molecules that affect Rho GTPase activity include growth factors, adhesion or guidance molecules, cytokines, neurotransmitters and other neuroactive molecules²⁵. Indeed, the decreases in growth rates seen with expression of mutant GTPase constructs in the absence of visual stimulation probably represent the effects of these other signalling pathways on GTPase-mediated regulation of cytoskeletal structure.

Little is known about the mechanisms that link synaptic activity to structural changes in dendrites. Previous studies have indicated that actin-based spine dynamics are regulated by glutamate receptor activity⁶ and that afferent activity promotes the formation of dendritic structures^{2,4,5,7} and the stabilization of synaptic contacts^{2,26}. Here, we show a direct relation between sensory input, glutamate-mediated synaptic activity and GTPase-mediated dendritic structural plasticity in the intact animal (Fig. 4e). Our observations demonstrate that the initiation and selective stabilization of new dendritic branches occur in response to a visual stimulus. Our results indicate that visual stimulation affects structural plasticity *in vivo*, through NMDA receptor-induced intracellular signalling events mediated by the Rho GTPases. □

Methods

Image acquisition

Tadpoles were anaesthetized with 0.02% 3-aminobenzoic acid ethyl ester (MS222, Sigma) in Steinberg's solution for all procedures. Single tectal neurons were labelled by iontophoresis of DiI³ or by electroporation with pEGFP-C1 (Clontech), or with pEGFP-C1 and recombinant EGFP-GTPase plasmids in a 4:1 (GTPase:GFP) ratio²⁷. Confocal images were collected through a $\times 40$ Nikon oil immersion lens (1.3 NA) at 2- μ m steps through the entire z-dimension of labelled neurons⁵. Two-photon images were collected at 1.5- μ m steps with a custom-built microscope based on a modified Olympus Fluoview confocal scan box mounted on an Olympus BX50WI microscope with a Tsunami femtosecond-pulsed Ti:Sapphire laser. We used an Olympus LUM Plan F1/IR $\times 40$ water immersion objective (0.8 NA). Two-photon optical sections were an average of three frames. For the experiment in which neurons were imaged every hour over 8 h, animals were returned to a dark chamber in between image collection during the first 4-h period. During the second 4-h period animals were returned to the chamber with the visual stimulus in between imaging sessions. Tadpoles recovered from anaesthetic between imaging sessions.

Visual stimulus

Albino *Xenopus laevis* tadpoles were reared in ambient light until stage 46–47. Tadpoles have a functional visual system from stage 39/40 onward, in which retinal ganglion cell axons make glutamate-receptor-mediated synaptic connections with dendrites of tectal cells²⁸. Retinal ganglion cells respond well to a light on/light off stimulus. A 2-s step of light on or off evokes synaptic currents in tectal cells of *Xenopus* tadpoles²⁸. On the basis of these response properties, freely swimming tadpoles were placed individually in wells of a 12-well plate in a black Plexiglas chamber with a 3×4 panel of green light-emitting diodes (LEDs; λ_{max} 567 nm, AND191GCP; Allied Electronics) on the top of the chamber. Each row of LEDs turned on and remained on for 1 s at a frequency of 0.2 Hz. The rows turned on and off sequentially to create a simulated motion stimulus, with 1 s of darkness between each cycle. *Xenopus* tadpole tectal cells can respond to repeated stimulation of the same region of retina without apparent adaptation²⁸. In our experiments, adaptation of tectal cells to the stimulus is not likely to be significant because the animals are swimming freely during the stimulation period, so the apparent location and direction of the stimulus vary constantly. Light exposure during the 4-h period in the absence of visual stimulation was kept to a minimum, but animals were exposed to some light during imaging. Some animals were exposed to 100 μ M DL-APV or 20 μ M CNQX during visual stimulation. MK801, another NMDA receptor antagonist, had a similar inhibitory effect on light-induced growth to that seen with APV (relative growth rate: 0.94 ± 0.73 , $n = 9$). Treatment of tectal cells with APV while the animals were in the dark for 4 h did not significantly affect dendritic growth (relative growth rate: 1.34 ± 0.5 , $n = 9$, $P = 0.7$).

Image analysis

We used a 4-h imaging protocol on the basis of our previous studies which showed that 4 h is sufficiently long to detect quantifiable increases in dendritic arbor branch length and branch-tip number, but short enough so that images of arbors from sequential time points can be reliably superimposed⁹. We measured the total dendritic branch length (TDBL) and branch-tip number of the dendritic arbors by reconstructing the whole dendritic arbor in

three dimensions using Object Image (<http://simon.bio.uva.nl/object-image.html>). The software computed the TDBL and branch-tip number using custom macros written by E.S.R.²⁹. Values are expressed as mean and standard error. Statistical analysis was done with Mann-Whitney *U* nonparametric statistical analysis and Wilcoxon signed-rank test. Analysis was performed blind to the type of treatment. Between 9 and 24 neurons per treatment were analysed, unless stated otherwise.

Construction of expression plasmids of GTPase mutants

Fragments (600 base pairs) containing the full coding sequence of RacN17, Cdc42N17, RhoAN19 and RhoV14 were cloned in-frame into pEGFP-C1 (Clontech Laboratories) and expressed as GFP-fusion proteins³⁰.

Received 10 April; accepted 25 June 2002; doi:10.1038/nature00987.

1. Builluart, P. et al. Oligophrenin-1 encodes a rhoGAP protein involved in X-linked mental retardation. *Nature* **392**, 823–826 (1998).
2. Engert, F. & Bonhoeffer, T. Dendritic spine changes associated with hippocampal long-term synaptic plasticity. *Nature* **399**, 66–70 (1999).
3. Li, Z., Aizenman, C. D. & Cline, H. T. Regulation of Rho GTPases by crosstalk and neuronal activity *in vivo*. *Neuron* **33**, 741–750 (2002).
4. Li, Z., Van Aelst, L. & Cline, H. T. Rho GTPases regulate distinct aspects of dendritic arbor growth in *Xenopus* central neurons *in vivo*. *Nature Neurosci.* **3**, 217–225 (2000).
5. Maletic-Savatic, M., Malinow, R. & Svoboda, K. Rapid dendritic morphogenesis in CA1 hippocampal dendrites induced by synaptic activity. *Science* **283**, 1923–1927 (1999).
6. Fischer, M., Kaech, S., Wagner, U., Brinkhaus, H. & Matus, A. Glutamate receptors regulate actin-based plasticity in dendritic spines. *Nature Neurosci.* **3**, 887–894 (2000).
7. Wong, W. T., Faulkner-Jones, B. E., Sanes, J. R. & Wong, R. O. Rapid dendritic remodeling in the developing retina: dependence on neurotransmission and reciprocal regulation by Rac and Rho. *J. Neurosci.* **20**, 5024–5036 (2000).
8. Wu, G.-Y., Zou, D. J., Rajan, I. & Cline, H. T. Dendritic dynamics *in vivo* change during neuronal maturation. *J. Neurosci.* **19**, 4472–4483 (1999).
9. Rajan, I. & Cline, H. T. Glutamate receptor activity is required for normal development of tectal cell dendrites *in vivo*. *J. Neurosci.* **18**, 7836–7846 (1998).
10. Van Aelst, L. & D'Souza-Schorey, C. Rho GTPases and signaling networks. *Genes Dev.* **11**, 2295–2322 (1997).
11. Luo, L. Rho GTPases in neuronal morphogenesis. *Nature Rev. Neurosci.* **1**, 173–180 (2000).
12. Penzes, P. et al. The neuronal Rho-GEF Kalirin-7 interacts with PDZ domain-containing proteins and regulates dendritic morphogenesis. *Neuron* **29**, 229–242 (2001).
13. Kim, J. H., Liao, D., Lau, L.-F. & Hagan, R. L. SynGAP: a synaptic RasGAP that associates with the PSD-95/SAP90 protein family. *Neuron* **20**, 683–691 (1998).
14. Zhang, W., Vazquez, L., Apperson, M. & Kennedy, M. B. Citron binds to PSD-95 at glutamatergic synapses on inhibitory neurons in the hippocampus. *J. Neurosci.* **19**, 96–108 (1999).
15. Furuyashiki, T. et al. Citron, a Rho-target, interacts with PSD-95/SAP-90 at glutamatergic synapses in the thalamus. *J. Neurosci.* **19**, 109–118 (1999).
16. Chen, H. J., Rojas, S. M., Oguni, A. & Kennedy, M. B. A synaptic Ras-GTPase activating protein (p135 SynGAP) inhibited by CaM kinase II. *Neuron* **20**, 895–904 (1998).
17. Lawler, S. Regulation of actin dynamics: the LIM kinase connection. *Curr. Biol.* **9**, R800–R802 (1999).
18. Aspenstrom, P. Effectors for the Rho GTPases. *Curr. Opin. Cell Biol.* **11**, 95–102 (1999).
19. Albertinazzi, C., Gilardelli, D., Paris, S., Longhi, R. & de Curtis, I. Overexpression of a neural-specific rho family GTPase, cRac1B, selectively induces enhanced neurite outgrowth and neurite branching in primary neurons. *J. Cell Biol.* **142**, 815–825 (1998).
20. Acebes, A. & Ferrus, A. Cellular and molecular features of axon collaterals and dendrites. *Trends Neurosci.* **23**, 557–565 (2000).
21. Debant, A. et al. The multidomain protein Trio binds the LAR transmembrane tyrosine phosphatase, contains a protein kinase domain, and has separate rac-specific and rho-specific guanine nucleotide exchange factor domains. *Proc. Natl Acad. Sci. USA* **93**, 5466–5471 (1996).
22. Wilk-Blaszczak, M. et al. The monomeric G-proteins Rac1 and/or Cdc42 are required for the inhibition of voltage-dependent calcium current by bradykinin. *J. Neurosci.* **17**, 4094–4100 (1997).
23. Djoudier, N., Prepens, U., Aktories, K. & Cavaliere, A. Inhibition of calcium release-activated calcium current by Rac/Cdc42-inactivating clostridial cytotoxins in RBL cells. *J. Biol. Chem.* **275**, 18732–18738 (2000).
24. Wu, G.-Y. & Cline, H. T. Stabilization of dendritic arbor structure *in vivo* by CaMKII. *Science* **279**, 222–226 (1998).
25. Kjoller, L. & Hall, A. Signaling to Rho GTPases. *Exp. Cell Res.* **253**, 166–179 (1999).
26. Lendvai, B., Stern, E. A., Chen, B. & Svoboda, K. Experience-dependent plasticity of dendritic spines in the developing rat barrel cortex *in vivo*. *Nature* **404**, 876–881 (2000).
27. Haas, K., Sin, W.-C., Javaherian, A., Li, Z. & Cline, H. T. Single-cell electroporation for *in vivo* neuronal gene expression. *Neuron* **29**, 1–9 (2001).
28. Zhang, L. I., Tao, H. W. & Poo, M. Visual input induces long-term potentiation of developing retinotectal synapses. *Nature Neurosci.* **3**, 708–715 (2000).
29. Ruthazer, E. S. & Cline, H. T. Multiphoton imaging of neurons in living tissue: acquisition and analysis of time-lapse morphological data. *J. Real-Time Imag.* **8**, 175–188 (2002).
30. Leung, T., Chen, X. Q., Manser, E. & Lim, L. The p160 RhoA-binding kinase ROK α is a member of a kinase family and is involved in the reorganization of the cytoskeleton. *Mol. Cell. Biol.* **16**, 5313–5327 (1996).

Supplementary Information accompanies the paper on Nature's website (<http://www.nature.com/nature>).

Acknowledgements

We thank K. Svoboda, P. O'Brien and B. Burbach for help constructing the two-photon microscope and P. O'Brien for constructing the electronic circuit for visual stimulation. We also thank K. Bronson for technical assistance, J. Duffy for assistance with the figures, and T. Leung and J. Dong for cDNA. We are grateful to L. Van Aelst for discussions, and

R. Malinow, J. Dubnau and members of the Cline laboratory for comments on the manuscript. This work was supported by the NIH (H.T.C., K.H., E.S.R.) and an endowment from the Charles Robertson Foundation to H.T.C..

Competing interests statement

The authors declare that they have no competing financial interests.

Correspondence and requests for materials should be addressed to H.C. (e-mail: cline@cshl.org).

ERAAP customizes peptides for MHC class I molecules in the endoplasmic reticulum

Thomas Serwold, Federico Gonzalez, Jennifer Kim, Richard Jacob & Nilabh Shastri

Division of Immunology, Department of Molecular and Cell Biology, University of California, Berkeley, California 94720-3200, USA

The ability of killer T cells carrying the CD8 antigen to detect tumours or intracellular pathogens requires an extensive display of antigenic peptides by major histocompatibility complex (MHC) class I molecules on the surface of potential target cells¹. These peptides are derived from almost all intracellular proteins and reveal the presence of foreign pathogens and mutations. How cells produce thousands of distinct peptides cleaved to the precise lengths required for binding different MHC class I molecules remains unknown^{2,3}. The peptides are cleaved from endogenously synthesized proteins by the proteasome in the cytoplasm^{4,5} and then trimmed by an unknown aminopeptidase in the endoplasmic reticulum (ER)^{6–8}. Here we identify ERAAP, the aminopeptidase associated with antigen processing in the ER. ERAAP has a broad substrate specificity, and its expression is strongly upregulated by interferon- γ . Reducing the expression of ERAAP through RNA interference prevents the trimming of peptides for MHC class I molecules in the ER and greatly reduces the expression of MHC class I molecules on the cell surface. Thus, ERAAP is the missing link between the products of cytosolic processing and the final peptides presented by MHC class I molecules on the cell surface.

To identify the ER aminopeptidase, we used detergent to solubilize microsomes from mouse liver and spleens. Ion exchange chromatography of solubilized microsomes showed a predominant peak of activity that was blocked by the aminopeptidase inhibitor leucinethiol (Fig. 1a). This activity was purified by several chromatographic steps (Methods). The highly enriched fractions from the final purification step contained one main band with a relative molecular mass (M_r) of roughly 100,000 (100K) on a SDS polyacrylamide gel electrophoresis (SDS–PAGE) gel stained with Coomassie blue (Fig. 1b). We subjected this band to in-gel trypsin digestion followed by matrix-assisted laser-desorption/ionization time-of-flight mass spectrometry and used the resulting tryptic peptide fingerprint to search the National Center for Biotechnology Information database^{9–11}.

In two independent experiments, 25 masses matched the predicted output of trypsin-digested murine adipocyte-derived leucine aminopeptidase (accession code AF227511)¹². This assignment was verified with the amino acid sequences of four peptides determined by high-energy collision-induced dissociation tandem mass spec-

trometry analysis (Fig. 1c)¹³. This murine aminopeptidase of 930 amino acids and its probable human and rat orthologues are also known as puromycin-insensitive leucyl-specific aminopeptidase^{12,14,15}. On the basis of our results, we hereafter refer to this enzyme as ERAAP (for ER aminopeptidase associated with antigen processing) to designate its intracellular location and function in trimming peptides in the MHC class I antigen processing pathway.

ERAAP is a member of the M1 family of zinc metalloproteases that are defined by a highly conserved His-Glu-X-X-His-X₁₈-Glu motif in the core peptidase unit (ref. 16 and Fig. 1c). The amino terminus contains a hydrophobic leader sequence, which indicated that it might be cotranslationally translocated into the ER. Hydrophobicity plots did not predict any other transmembrane domains, and there were no other obvious motifs to predict its intracellular location. To determine its location, therefore, we first transfected COS cells with the murine ERAAP complementary DNA and carried out western blot analysis with the whole-cell lysates and the culture supernatants. A single band close to the predicted

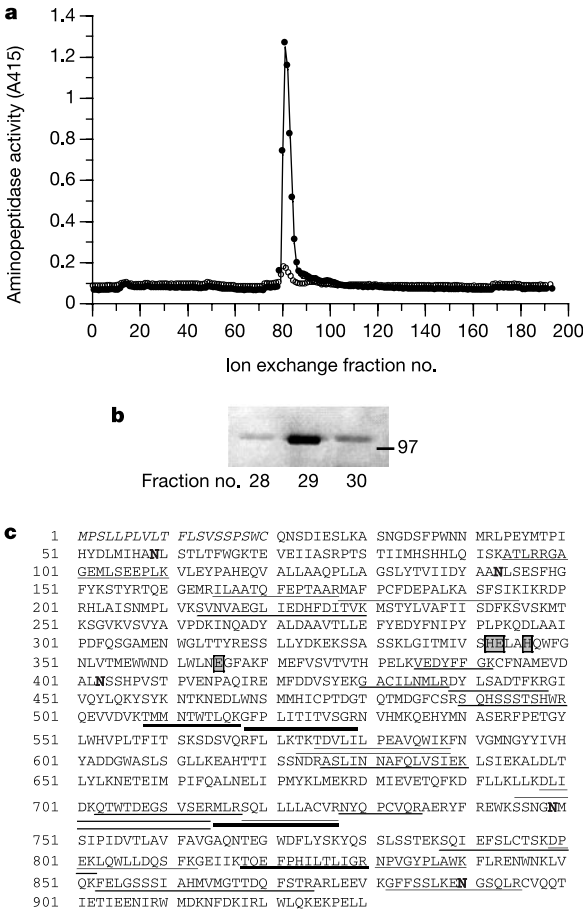


Figure 1 Purification and identification of ERAAP. **a**, Microsomes from mouse livers and spleens were lysed in detergent and separated by ion exchange chromatography. Fractions were tested for aminopeptidase activity by incubating with leucine *p* nitroanilide without (filled circles) or with (open circles) the aminopeptidase inhibitor leucinethiol. **b**, SDS–PAGE gel stained with Coomassie blue of three consecutive fractions containing aminopeptidase activity from the final hydrophobic interaction chromatography purification step. **c**, The sequence of murine ERAAP. Underlined peptides matched the masses identified by mass spectrometry. Peptides identified by sequencing are underlined in bold. The ER translocation signal at the N terminus is in italics, active-site residues are boxed, and putative *N*-linked glycosylation sites are in bold.